Civil Engineering and Applied Solutions

Research Article

journal homepage: ceas.journals.umz.ac.ir

CEAS Civil Engineering and Applied Solutions

Dynamic Analysis of Fatigue-Cracked Beams: The Nonlinear Response with the Analytical Method

Ali Asgari [a*], Alireza Khabiri [a]

[a] *Department of Civil Engineering, Faculty of Engineering and Technology, University of Mazandaran, Babolsar, Iran*

ARTICLE INFO

Keywords:
Fatigue beam
Cracked beam
Breathing crack
Nonlinear response
Damping ratio

Article history:
Received 21 April 2025
Accepted 12 May 2025
Available online 01 July 2025

ABSTRACT

In this study, the bending vibration of a fatigue-cracked beam and associated constraint conditions have been solved by implementing the Homotopy Perturbation Method. A structure with a single degree of freedom, varying stiffness, and a periodic function is employed to simulate the dynamic behavior of the beam. The crack is represented as an ongoing disturbance function within the displacement field, which could be obtained from fracture mechanics. The governing equation's solution shows the super harmonics of the dominant frequency, resulting from nonlinear impacts on the dynamic vibration response of the cracked beam. The proposed method gives an analytical closed-form solution that can be easily used to analyze and design structures dynamically. The outcomes show that growing crack depth reduces the natural frequencies of a cracked beam. Moreover, increasing the severity of the crack and moving its location toward the center of the beam increases the system's damping. Perturbation methods rely on a small parameter, which is challenging to determine for real-life nonlinear problems. To overcome this shortcoming, a powerful analytical method is introduced to solve the motion equation of the cracked beam.

1. Introduction

Mathematical modeling of beams and frames, incorporating various theories and effects, is a vital study area within structural engineering [1, 2]. This applied topic plays a crucial role in understanding and predicting the behavior of structural components under diverse loading conditions [3]. Numerous scientific issues and phenomena, including the vibration of a beam with fatigue cracks, occur in nonlinear models [4-6]. Identifying analytical solutions for these problems is challenging. Cracks are typically detected using a nonlinear approach that monitors variations in the dynamic response features, like natural frequencies, damping, and mode shapes [7–9]. In the analysis of linear vibrations in a cracked beam, the beam crack is assumed to stay open during the beam's vibrations [10, 11]. These linear vibration methods often fail to produce practical results due to low defect sensitivity. Ke et al. [12] examined how open-edge crack parameters affect free vibration and buckling features of cracked beams composed of functionally graded materials. The nonlinear performance of a cantilevered cracked beam modeled with bilinear stiffness under harmonic excitation was investigated to deliberate the crack closure effects [13, 14]. Kisa and Brandon [15] employed a bilinear stiffness model to assess the variations in beam stiffness at the crack position. They presented the contact flexural stiffness matrix within a finite element (FE) model to effectively simulate the impact of crack closure, which was integrated into the initial flexural stiffness matrix at the crack site during a half-cycle of shaking. This stiffness matrix deliberates only two conditions: entirely open and entirely closed states of the crack. Under this assumption, the assumed cracked beam exhibits just dual stiffness values: a more significant value for the closed crack state and a smaller value for the wide crack state. This approach suggests that the crack expands and contracts instantaneously. The experimental tests show that the transition between closed and open cracks, and contrarily, happens more smoothly [16]. Abraham and Brandon [17] have modeled the changes in stiffness at the position of the breathing crack by using several expressions of the Fourier transform series.

* Corresponding author.
E-mail addresses: a.asgari@umz.ac.ir (A. Asgari).

https://doi.org/10.22080/ceas.2025.29000.1002.
ISSN: 3092-7749/
How to cite this article: Asgari, A., Khabiri, A. Dynamic analysis of fatigue-cracked beams: the nonlinear response with the analytical method. Civil Engineering and Applied Solutions. 2025; 1(2): 43-54. doi:10.22080/ceas.2025.29000.1002.

Cheng et al. [18] have examined a single degree of freedom (SDOF) cracked cantilever beam through time-varying stiffness to investigate frequency-forced vibration behavior. The time-varying stiffness of the beam is shown as a regular periodic function. They presumed that the damping ratio of the flexural cracked beam is 0.01 and obtained forced vibration responses of the cracked beam through the numerical Runge-Kutta technique. Likewise, they stated that using an open crack model for crack detection does not provide high accuracy in monitoring fundamental frequency and tends to underestimate the severity of the crack. Following a similar methodology, Ariaei et al. announced a technique to assess the dynamic Euler-Bernoulli undamped beams with the effect of breathing cracks subjected to a moving point mass [19]. This approach utilizes the discrete element technique in conjunction with the FE method. Researchers have similarly employed signal processing methods to establish the above-mentioned model for beam crack detection [20, 21]. Zhang and Testa experimentally explored the closure properties of the vibration response of a fatigue-cracked T-style steel structure [22]. Bovsunovsky and Surace investigated the super harmonic vibration of a flexural cracked cantilever beam caused by the nonlinear effects of crack closure [23]. They clarified that these nonlinear effects create considerable challenges in achieving analytical solutions. Consequently, they employed a FE model, enabling the prediction of alterations in damping due to the cracked beam. They exhibited that nonlinear effects in the vibration response depend on the crack parameters and the damping scale in the vibrating system. In another work, Curadelli et al. employed changes in system damping to identify structural damage through wavelet analysis [24]. Dimarogonas provided valuable, detailed surveys on crack modeling approaches, emphasizing the importance of utilizing practical numerical models in the diagnostic method [25]. The cracked beam's analytical response presents valuable physical insights into the issue at hand, allowing for an easy assessment of how all parameters affect the solution. Rezaee and Hassan Nejad [26] applied an analytical method, the perturbation method, to solve the motion equation of a cracked beam. They demonstrated that the dynamic response of the cracked beam takes the form of an exponential function and a nonlinear oscillatory behavior function. The exponential part of the reaction introduces the decay rate due to the system damping, and the oscillatory portion is the solution of the Mathieu formula, showing super harmonics of the beam's dominant frequency. They also showed that the system response's damping rate can be derived from the constants of the Mathieu equation.

A recent study of contemporary structural health monitoring evaluates infrastructure using high-resolution imaging techniques to identify and measure defects like cracks. Structural engineers rely on this data to refine structural models and assess the safety and integrity of the structures. The practical use of cracked beams is a critical indicator of structural integrity in various applications. By monitoring cracks in beams, engineers can assess the extent of deterioration over time. This is particularly important in civil engineering, where infrastructure such as bridges and buildings must remain safe and functional. Regularly monitoring cracked beams enables timely maintenance interventions and helps prevent catastrophic failures. Additionally, data gathered from cracked beams can inform predictive maintenance strategies, ensuring that resources are allocated efficiently and that infrastructure remains reliable for public use [27]. An experimental study examined the relationship between crack propagation and deflection in reinforced concrete beams. A four-point loading test was conducted on specimens with varied reinforcement ratios and concrete cover thicknesses [28].

As is well known, perturbation methods rely on a small parameter, which is often challenging to determine for real-life nonlinear phenomena problems. In this paper, to overcome this shortcoming, a novel, robust analytical technique is presented to solve the governing equation (GE) of motion of the fatigue-cracked beam. The Homotopy Perturbation Method (HPM) deforms a complex problem and turns it into an easily solvable issue. The analytical results for a specified case are compared with typical experimental and numerical methods to validate. This method gives an analytical solution for the nonlinear cracked beam equation, which does not need meshing like the numerical method. Also, this method's result is proposed in the closed-form formula, which can be easily used for further structural evaluations.

2. Mathematical modeling

In practical terms, cracked beams are central to a wide range of applications, from ensuring safety in infrastructure and buildings to informing design processes and enhancing material performance. Understanding cracked beams allows engineers and construction professionals to make informed decisions that improve safety and longevity. According to beam crack modeling, the model conforms to the Euler-Bernoulli assumptions and is excited in its first frequency mode. This assumption is valid when the beam is subject to the initial mode by ignoring the contributions of the higher modes.

This mathematical modeling introduces a practical and credible model for examining the nonlinear dynamic characteristics of an SDOF fatigue-cracked beam. The beam's equivalent mass is located at its center in this model. For better visualization, see the beam's stiffness by the variations in location and depth of the crack (see Fig. 1). Consequently, the disparity of the flexibility of the beam as a result of the crack is assessed. Then, the change in the equivalent stiffness of the fatigue-cracked section through the vibration is assumed to be a time-varying function. However, the lumped parameters of the structure are decisive.

2.1. Assess the flexibility of a beam supported by pins with a crack

Assuming a bending moment is exerted on a fatigue-cracked beam, it will also experience additional rotation due to the crack. The extra rotation at the crack position is proportional to the beam flexure. According to Castigliano's theorem, U_T is the crack's strain energy, and the additional rotation takes the following form [29]:

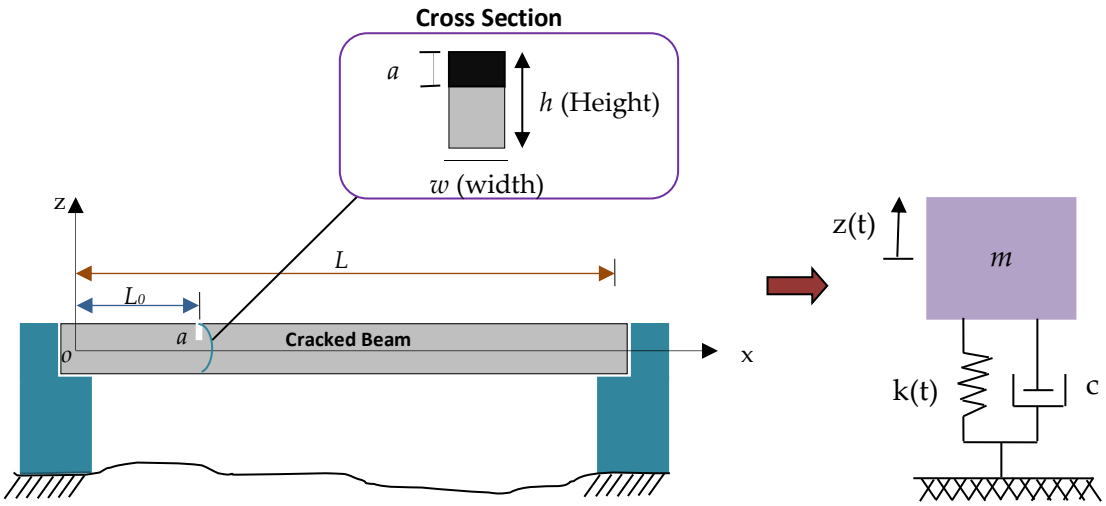

Fig. 1. (a) The pinned-supported fatigue-Cracked beam with a specified damage location, and (b) The schematic SDOF mass, spring, and damping model.

$$\theta = \frac{\partial U_T}{\partial M} \tag{1}$$

The strain energy is presented in the form below [30]:

$$U_T = \int_{Crack} \varsigma_s(\alpha) d\alpha \tag{2}$$

This equation is called the Paries' Equation. The integral in Eq. 2 is an integral over a surface as follows [23]:

$$U_T = \int_{-\frac{w}{2}}^{\frac{w}{2}} \int_0^a \varsigma_s(\alpha) d\alpha dy \tag{3}$$

where the crack depth notation is a, also ς_s is the strain energy density, obtainable from the subsequent equation [31]:

$$\text{Plane strain: } \varsigma_s = \frac{1-\nu^2}{E}\left[K_I^2 + K_{II}^2 + \frac{K_{III}^2}{1-\nu}\right]$$
$$\text{Plane stress: } \varsigma_s = \frac{1}{E}[K_I^2 + K_{II}^2 + (1+\nu)K_{III}^2] \tag{4}$$

In the above formulas E and νrespectively are Young's modulus and Poisson's ratio. In this paper, the plain strain assumption is used. In addition, in Eq. 4, K_I, K_{II},and K_{III} are the Stress Intensity Factors (SIF) related to the fracture modes. In fracture mechanics, the SIF are established for a beam of unit thickness containing a transverse crack [22]. The intensity of stress concerning a single-edge crack under pure bending is:

$$K_I = \sigma_0 \sqrt{\pi a} F_I\left(\frac{a}{h}\right) \tag{5}$$

$$\sigma_0 = \frac{6M}{wh^2} \tag{6}$$

$$\varsigma_s = \frac{1-\nu^2}{E}\sigma_0^2 \pi a F_I^2(\alpha),\ F_I(\alpha) = 1.12 - 1.4\alpha + 7.33\alpha^2 - 13.4\,\alpha^3 + 14\,\alpha^4 \tag{7}$$

By substituting Eq. 7 into Eq. 3 and integrating over the crack surface, the amount of the strain energy U_T can be obtained as:

$$U_T = \frac{36\,\pi\,(1-\nu^2)}{E}\frac{M^2}{wh^2} g(\alpha) \tag{8}$$

where

$$g(\alpha) = 19.6\,\alpha^{10} - 40.7556\,\alpha^9 + 47.1063\,\alpha^8 - 33.051\,\alpha^7 + 20.2948\,\alpha^6 - 9.9736\,\alpha^5 + 4.5948\,\alpha^4 - 1.04533\,\alpha^3 + 0.6272\,\alpha^2 \tag{9}$$

Conversely, the alterations in the beam's flexibility produced by the crack resulted from the formula presented by Dimarogonas and Paipatis [29]:

$$\Delta C = \frac{\partial^2 U_T}{\partial P^2} = \frac{18\,L_0^2 \pi (1-\nu^2)}{Ewh^2} g(\alpha) \tag{10}$$

This equation calculates the changes in flexibility of a pinned-supported beam caused by the crack.

2.2. Finding the motion GE

Assume a uniform pinned-supported beam with a length L, which is shown in Fig. 1. The crack depth is presented as a, and it is situated at a distance of L_0 from the beam's left end. The beam cross-section's width and height are w and h, respectively. It is assumed that the beam vibrates at its fundamental frequency mode. So, the flexurally fatigued cracked beam can be modeled as an SDOF. The crack is modeled as a fatigue crack with breathing behaviors. Henceforward, the beam stiffness will change through the vibration caused by the crack's opening and closing, and the beam's dynamic response will have a nonlinear characteristic.

To achieve the equivalent mass and stiffness of the system, the initial mode shape of the beam is considered to take the form below [32]:

$$\Phi(x) = sin\left(\frac{\pi x}{L}\right) \tag{11}$$

Additionally, the beam stiffness for the scenario of an entirely closed crack is provided by [33]:

$$k_c = \frac{1}{C} = \int_0^L EI\, \Phi''^2(x)\, dx = \frac{\pi^4 EI}{2L^3} \tag{12}$$

where k_c and C represent the stiffness and flexibility of the fatigue-cracked beam once the crack is completely closed, EI is the bending rigidity. Additionally, the notation of the beam's stiffness once the crack model is completely open is $k_o = 1/C_o$, and C_o is the flexibility for the completely open beam's crack as:

$$C_0 = C + \Delta C \tag{13}$$

As previously noted, the flexural Fatigue-Cracked beam's vibration changes the system's equivalent stiffness due to the crack's opening and closing. Thus, the following time-varying function can be employed to model the equivalent stiffness variations of the SDOF structure[19]:

$$k(t) = k_0 + k_{\Delta c}\,[1 + cos(\omega_b t)] \tag{14}$$

In the above formula, $k_{\Delta c}$ represents the amplitude of changes in equivalent stiffness in the following form:

$$k_{\Delta c} = \frac{1}{2}(k_c - k_o) \tag{15}$$

Eq. 14 states that the cracked beam at the static equilibrium position of the beam has a stiffness that represents the average of the maximum stiffness values for both entirely open and entirely closed crack scenarios. Consequently, as the beam vibrates and moves up and down around its equilibrium position, its equivalent stiffness fluctuates around this average value. It is logical to assume that when the beam is displaced in the direction that begins to open the crack, its stiffness gradually decreases; conversely, moving the beam in the opposite direction continuously increases stiffness. In Eq. 14, ω_b is the crack breathing frequency, and for the case of a fully closed crack, $(k(t) = k_c)$, we have $\omega_b t = 2\,n\,\pi,\, n = 1,2,3,\ldots$. and for the case of a fully open crack $(k(t) = k_0)$, we have $\omega_b t = (2\,n - 1)\,\pi, n = 1,2,3,\ldots$. The breathing frequency can be approximated as [34]:

$$\omega_b = \frac{2\omega_c\omega_o}{\omega_c+\omega_o} \tag{16}$$

where $\omega_o = \sqrt{k_o/m}$, and $\omega_c = \sqrt{k_c/m}$ are the frequencies of the cracks that relate to completely open and closed crack cases. Eq. 16 suggests that the system's dominant frequency consistently lies between the open and closed crack cases.

In the above equations, the fraction $m\omega_b^2$ can be written in terms of k_c and k_o as:

$$m\omega_b^2 = \frac{4\,k_o k_c}{k_o+k_c+2\sqrt{k_o k_c}} \tag{17}$$

In addition, to determine the beam's equivalent mass, one could proceed as follows:

$$m = \int_0^L m(x)\,\Phi^2(x)dx = 0.5\,\bar{m}L \tag{18}$$

The mass per unit length of the beam is $\bar{m}$. Taking into account c as the damping equivalent coefficient for the SDOF model of the damaged beam (refer to Fig. 1) and integrating the lumped modal parameters such as equivalent mass and time-varying flexural stiffness, we derive the GE of motion as:

$$m\ddot{z} + c\dot{z} + \{k_o + k_{\Delta c}[1 + cos(\omega_b t)]\}z = 0 \tag{19}$$

An analytical solution for the equation mentioned above has not been reported, and there are numerical solutions that assume a constant damping coefficient [18].

By utilizing the subsequent variable change:

$$t = \frac{2\tau}{\omega_b},\ \frac{dz}{dt} = \frac{\omega_b}{2}\frac{dz}{d\tau},\ \frac{d^2z}{dt^2} = \frac{\omega_b^2}{4}\frac{d^2z}{d\tau^2} \tag{20}$$

and replacing the above relations into Eq. 19, and dividing Eq. 19 by $\frac{4\,m}{\omega_b^2}$ and rearranging the equation, it becomes:

$$\frac{d^2z(\tau)}{d\tau^2} + 4\xi\frac{dz(\tau)}{d\tau} + [\delta + 4\xi^2 + 2\varepsilon\,cos(2\tau)]\,z(\tau) = 0 \tag{21}$$

where, δ, ε and ξ are non-dimensional parameters and damping ratio, respectively, which are defined as:

$$\varepsilon = \frac{2k_{\Delta C}}{m\,\omega_b^2} = \frac{k_c - k_o}{m\,\omega_b^2}, \xi = \frac{c}{2\,m\,\omega_b}, \delta = \frac{4\,(k_o - k_{\Delta C})}{m\,\omega_b^2} - 4\,\xi^2 = \frac{2(k_o + k_c)}{m\omega_b^2} - 4\xi^2 \tag{22}$$

This equation exhibits a stable periodic solution when δ is expressed in terms of ε (with ε being much less than 1) as:

$$\delta = \sum_{i=0}^{\infty} G_i p^i \tag{23}$$

where G_0 is an integer number (G_0 = 0, 1, 2, …) and $p \in [0,1]$ is an embedding parameter, and $G_i (i = 1,2,3,\ldots,\infty)$ represented as the unknown expansion coefficients, which will be determined later. For each value of G_0 one can acquire the corresponding expansion coefficients, thus, the associated transition curves. Each individual point on the curves represents a stable and periodic result to Eq. 21 (Fig. 2). In this illustration, the hatched regions indicate the unstable areas.

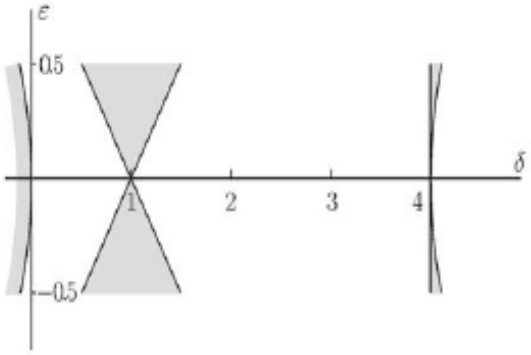

Fig. 2. The Transition curves distinguish among the regions of stability and instability plane. The hatched areas represent the unstable region [34].

By substituting Eq. 17 into Eq. 22, and using relations $k_o = 1/C_o$ and $k_c = 1/C$, ε and δ are obtained as:

$$\varepsilon = \frac{\chi^2 + 2\chi(1+\sqrt{1+\chi})}{4(1+\chi)},\ \chi = \frac{\Delta C}{C} \tag{24}$$

$$\delta = \frac{8 + 2\,\chi^2 + 8\,\chi + 4\,(2+\chi)(\sqrt{1+\chi})}{4\,(1+\chi)} - 4\,\xi^2 \tag{25}$$

It's evident from Eq. 24 and 25 that ε and δ are functions of χ and the damping ratio denoted by ξ. For a periodic result to the motion equation (Eq. 21), the $\varepsilon - \delta$ curve needs to align via a transition curve. Then, the variation limits of χ should be established since the Mathieu equation features a periodic solution.

3. The HPM for solving the motion equation

An analytical relation exists between a cracked beam's damping ratio and crack parameters. This division presents an analytical method for the free vibration of the supported beam. The initial conditions used for the solution of Eq. 21 are regarded as $z(0) = 1$ and $\dot{z}(0) = 0$. The initial conditions relate to the deformation of the equivalent mass from its equilibrium position by a distance of A, and the primary velocity of $-Ac/2m$.

As noted in the previous section, the Motion equation should have a periodic solution any time δ can be expressed in terms of ε as stated by Eq. 23. In Fig. 2, G_0 should be equal to 2.

In this letter, we apply the HPM to solve the discussed problem. The structure of the HPM is shown as follows:

$$(v,p) = L(v) - L(z_0) + pL(z_0) + p[N(v) - f(r)] = 0, \tag{26}$$

The notations $v(r,p)$: $\Omega \times [0,1] \to R$, L represents the linear, N represents the nonlinear part of the differential equation and $f(\tau)$ is a known analytical function.

Considering Eq. 26 we have:

$$H(v,0) = L(v) - L(z_0) = 0,\ H(v,1) = L(v) + N(v) - f(r) = 0 \tag{27}$$

In that $p \in [0,1]$ is an embedding parameter and z_0 is the initial estimate that satisfies the B.C. By substituting Eq. 21 into Eq. 26, it becomes:

$$H(v,p) = [\frac{d^2v(\tau)}{d\tau^2} + 4\,\xi\,\frac{dv(\tau)}{d\tau} + [\delta + 4\,\xi^2]v(\tau) - L(z_0)] + pL(z_0) + 2\,p\varepsilon\,cos(2\,\tau)\,v(\tau)] = 0, \quad (28)$$

The procedure for the changes in p from 0 to unity is $v(\tau, p)$, which changing from z_0 to z_r. z is considered as:

$$v(\tau) = \sum_{i=0}^{\infty} v_i(\tau)p^i \quad (29)$$

The most accurate estimate for the solution is:

$$z(\tau) = \lim_{p\to 1} \sum_{i=0}^{\infty} v_i(\tau)p^i \quad (30)$$

Inserting Eqs. 23 and 29 into Eq. 28 yields:

$$H(v,p) = [\sum_{i=0}^{\infty} \ddot{v}_i(\tau)p^i + 4\,\xi \sum_{i=0}^{\infty} \dot{v}_i(\tau)p^i + [\sum_{i=0}^{\infty} G_i p^i + 4\,\xi^2] \sum_{i=0}^{\infty} v_i(\tau)p^i - L(z_0)] + pL(z_0) + [2\,\varepsilon\,cos(2\,\tau)] \sum_{i=0}^{\infty} v_i(\tau)p^i] = 0, \quad (31)$$

Assuming $L(z_0) = 0$ and simplification and rearranging based on powers of p-terms and setting the coefficients to each power of p equal to 0 would result in an infinite collection of differential equations as:

$$p^0: \ddot{v}_0(\tau) + 4\,\xi\dot{v}_0(\tau) + (4\,\xi^2 + 4)v_0(\tau) = 0, v_0(0) = 1, \dot{v}_0(0) = 0 \quad (32\text{-}1)$$

$$p^1: \ddot{v}_1(\tau) + 4\xi\dot{v}_1(\tau) + (4\xi^2 + 4)v_1(\tau) = (2\varepsilon - G_1 - 4\varepsilon\,cos^2(\tau))v_0(\tau), v_1(0) = 0,\ \dot{v}_1(0) = 0 \quad (32\text{-}2)$$

$$p^2: \ddot{v}_2(\tau) + 4\xi\dot{v}_2(\tau) + (4\xi^2 + 4)\,v_2(\tau) = (2\varepsilon - G_1 - 4\varepsilon\,cos^2(\tau))z_1(\tau) - G_2v_0(\tau), v_2(0) = 0, \dot{v}_2(0) = 0 \quad (32\text{-}3)$$

$$p^3: \ddot{v}_3(\tau) + 4\,\xi\dot{v}_3(\tau) + (4\xi^2 + 4)v_3(\tau) = (2\,\varepsilon - G_1 - 4\,\varepsilon\,cos^2(\tau))v_2(\tau) - G_2v_1(\tau) - G_3v_0(\tau), v_3(0) = 0, \dot{v}_3(0) = 0 \quad (32\text{-}4)$$

The infinite set outlined in Eq. 32 has been solved recursively. To derive solutions for this set of equations, certain conditions must be placed on G_i . The first part of this set provides the zero-order estimate for the solution:

$$v_0(\tau) = e^{-2\xi\tau}(A_0\,sin(2\tau) + B_0\,cos(2\tau)) \quad (33)$$

The constants $A_0$and B_0in Eq. 33 are assessed by applying the initial conditions. Solving Eq. 32-1 and taking into account suitable initial conditions, gives $v_0(\tau) = e^{-2\xi\tau}\,cos(2\tau)$. Using Eq. 32-2, we have

$$v_1(\tau) = \varepsilon e^{-2\xi\tau}\left(-\frac{1}{3} + \frac{1}{6}cos(2\tau) + \frac{1}{6}cos^2(2\tau) - \frac{1}{4}G_1\tau\,sin(2\tau)\right) \quad (34)$$

To meet the periodicity conditions for $v_0(\tau)$, G_1 is equal to zero. Henceforward, the answer to the second part of Eq. 32 is:

$$v_1(\tau) = \varepsilon e^{-2\xi\tau}\left(-\frac{1}{3} + \frac{1}{6}cos(2\tau) + \frac{1}{6}cos^2(2\tau)\right) \quad (35)$$

Knowing that $G_1 = 0$, and using Eq. 32-3, $v_2(\tau)$ is obtained in the following form:

$$v_2(\tau) = \frac{1}{288}e^{-2\xi\tau}(3\varepsilon^2\,cos^3(2\tau) + 8\varepsilon^2\,cos^2(2\tau) + 5\varepsilon^2\,cos(2\tau) + 30\left(\varepsilon^2 - \frac{12}{5}G_2\right)\tau\,sin(2\tau) - 16\,\varepsilon^2\right) \quad (36)$$

$v_2(\tau)$ will be periodic when the term's coefficient is set equal to zero, so $G_2 = 5/12\,\varepsilon^2$. Thus, similar procedures can be used; other equations of Eq. 32 can be solved recursively.

$$v_3(\tau) = \frac{1}{2880}e^{-2\xi\tau}(\varepsilon^3\,cos^4(2\tau) + 5\,\varepsilon^3\,cos^3(2\tau) + 29\,\varepsilon^3\,cos^2(2\tau) - 77\,\varepsilon^3\,cos(2\tau) - 720\,G_3\,\tau\,sin(2\tau) + 42\,\varepsilon^3), \quad G_3 = 0 \quad (37)$$

$$v_4(\tau) = \frac{1}{1658880}e^{-2\xi\tau}(12\,\varepsilon^4\,cos^5(2\tau) + 96\,\varepsilon^4\,cos^4(2\tau) + 1299\,\varepsilon^4\,cos^3(2\tau) - 5408\,\varepsilon^4\,cos^2(2\tau) - 16415\,\varepsilon^4\,cos(2\tau) - 22890\left(\frac{13824}{763}G_4 + \varepsilon^4\right)\tau\,sin(4\tau) + 20416\,\varepsilon^4), \quad G_4 = -\frac{763}{13824}\varepsilon^4 \quad (38)$$

$$v_5(\tau) = \frac{1}{116121600}e^{-2\xi\tau}(12\,\varepsilon^5\,cos^6(2\tau) + 140\varepsilon^5\,cos^5(2\tau) + 3335\,\varepsilon^5\,cos^4(2\tau) - 20685\,\varepsilon^5\,cos^3(2\tau) - 226585\,\varepsilon^5\,cos^2(2\tau) + 501113\,\varepsilon^5\,cos(2\tau) - 29030400\,G_5\tau\,sin(2\tau) - 257330\,\varepsilon^5), G_5 = 0 \quad (39)$$

Continuing with this process results in additional terms of $v_i(\tau)$, a few first terms will ensure suitable precision for the solution, and the other terms make a minor impact on the solution. By using a variable transformation $\tau = \omega_b t/2$ and $p \to 1$, the solution

for Eq. 19 in relations of ω_b at the actual time t is achieved:

$$z(t) = e^{-\frac{c}{2m}t}\Big[cos(\omega_b t) + \frac{1}{6}\varepsilon(cos^2(\omega_b t) + cos(\omega_b t) - 2) + \frac{1}{288}\varepsilon^2(3\,cos^3(\omega_b t) + 8\,cos^2(\omega_b t) + 5\,cos(\omega_b t) - 16) + \frac{1}{2880}\varepsilon^3(cos^4(\omega_b t) + 5\,cos^3(\omega_b t) + 29\,cos^2(\omega_b t) - 77\,cos(\omega_b t) + 42) + \frac{1}{1658880}\varepsilon^4\Big(12\,cos^5(\omega_b t) + 96\,cos^4(\omega_b t) + 1299\,cos^3(\omega_b t) - 5408\,cos^2(\omega_b t) - 16415\,cos(\omega_b t) + 20416 + \frac{1}{116121600}\varepsilon^5(12\,cos^7(\omega_b t) + 140\,cos^5(\omega_b t) + 3335\,cos^4(\omega_b t)\Big) - 20685\,cos^3(\omega_b t) - 226585\,cos^2(\omega_b t) + 501113\,cos(\omega_b t) - 257330 + \frac{1}{58060800}\varepsilon^6(72\,cos^7(\omega_b t) + 1152\,cos^6(\omega_b t) + 4224\,cos^5(\omega_b t)\Big) - 367968\,cos^4(\omega_b t) - 8571195\,cos^3(\omega_b t) + 30518176\,cos^2(\omega_b t) + 176434669\,cos(\omega_b t) - 198057152) + \dots.\Big] \quad (40)$$

, and

$$\delta = 4 + \frac{5}{12}\varepsilon^2 - \frac{763}{13824}\varepsilon^4 + \frac{1002401}{79626240}\varepsilon^6 - \frac{1669068401}{458647142400}\varepsilon^8 + \dots. \quad (41)$$

Eq. 41 has a clear physical interpretation. Eq. 22 shows δ , which is a function of the SDOF model parameters, breathing frequency, and the structural stiffness modifications caused by the crack. Also, Eq. (41) formulates δ in terms of ε for a periodic solution of D.E. (Eq. 21).

Thus, applying Eq. 25 alongside Eq. 41 establishes a relationship for the damping ratio of the fatigue-cracked beam based on its geometric dimensions, mechanical properties, and crack characteristics, as follows

$$\xi = \frac{1}{3317760}\frac{1}{1+\chi}(\sqrt{6}((1+\chi)(-917294284800 - 917294284800\chi - 191102976000\,\varepsilon^2 - 191102976000\,\varepsilon^2\chi + 25314508800\,\varepsilon^4 + 253145088000\,\varepsilon^4\chi - 5773829760\,\varepsilon^6 - 5773829760\,\varepsilon^6\chi + 1669068401\,\varepsilon^8 + 1669068401\,\varepsilon^8\chi + 229323571200\,\chi^2 + 917294284800\sqrt{1+\chi} + 458647142400\sqrt{1+\chi}\chi))^{1/2}) \quad (42)$$

where ε is a function of χ (See: Eq. 22). The Motion equation has an analytical and periodic solution only if δ and ε parameters of Eq. 21)are situated on the transition curves. An unbounded solution exists for any plane and location in the unstable region (highlighted sections in Fig. 2). Nonetheless, considering the cited crack's physical evidence, beam ε is always positive, and the associated transition curve $\delta - \varepsilon$ emanates from the point $\delta = 4$ on the δ axis. It is illustrated that when ε approaches zero, the precision of the asymptotic response will rise. Thus, utilizing Eq. 24, which illustrates the relationship between ε and χ, it is observed that when χ is less than 1.5, the value of ε will always be below unity. The formula between χ and the mechanical properties of the considered flexural fatigue-cracked beam takes the dimensionless form:

$$\chi = \frac{\Delta C}{C} = \frac{3\pi^5(1-\nu^2)}{4}\left(\frac{L_0}{L}\right)^2\left(\frac{h}{L}\right)g(\alpha) \quad (43)$$

Utilizing this dimensionless equation, χ can plot against the crack depth ratio $\alpha = a/h$, and the crack location ratio $\beta = L_0/L$ to establish the valid domain of the solution. The region of $\chi > 1.5$ is valid for the analytical solution. This method enables the derivation of the analytical solution for the free vibration response. Additionally, the beam's damping ratio can be computed based on the specified geometric dimensions, mechanical characteristics, and crack depth.

4. Results and discussion

Using the HPM outlined in section 3, this study investigates both the quantitative and qualitative parameters affecting the behavior of a fatigue-cracked beam. To compare the proposed method's results and the experimental findings reported in the reference [34], an aluminum pinned-supported with a length of 235 mm and a cross-sectional area of 7×23 mm^2 serves as a case example in this study. The material density and Young's modulus of elasticity of the beam are 2800 kg/m^3 and 72 GPa. As mentioned in section 2.2, the stiffness of a beam with a fatigue crack varies continuously over time as the beam vibrates, i.e., during each half-cycle of beam vibration, the stiffness of the beam transitions smoothly between the two extremes that represent a fully open crack and a fully closed crack case. Fig. 3 illustrates the change in stiffness overtime during a half-cycle vibration for a beam with a crack position ratio β = 0.2 and variable crack depth ratios of α. In this figure, the extreme values of the curve relate to entirely closed cases of the crack (i.e., the unaltered beam), and the lowest values relate to completely open cases of the crack. Additionally, this figure shows that a deeper crack leads to a broader range of stiffness variations, consequently decreasing the dominant frequency.

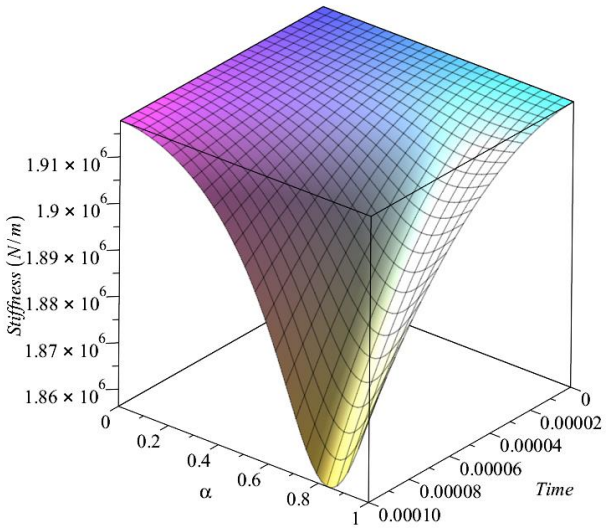

Fig. 3. The fatigue-Cracked beam's stiffness changes over time(s) with the position ratio for β = 0.2 and various crack depth ratios.

The recommended analytical method can assess a fatigue-cracked beam's free deformation and acceleration results for a specified crack depth and position. The computed free vibration responses of the fatigue-cracked beam for the crack parameters illustrated in Fig. 3 are presented in Figs. 4 and 5. In both scenarios, the initial deformation is z (0) = 1 cm. These figures indicate that greater crack depth results in a more significant decay of the fatigue-cracked beam's response. The emergence of the dominant frequency's super harmonics results from variations in the stiffness of the fatigue-cracked beam during vibration.

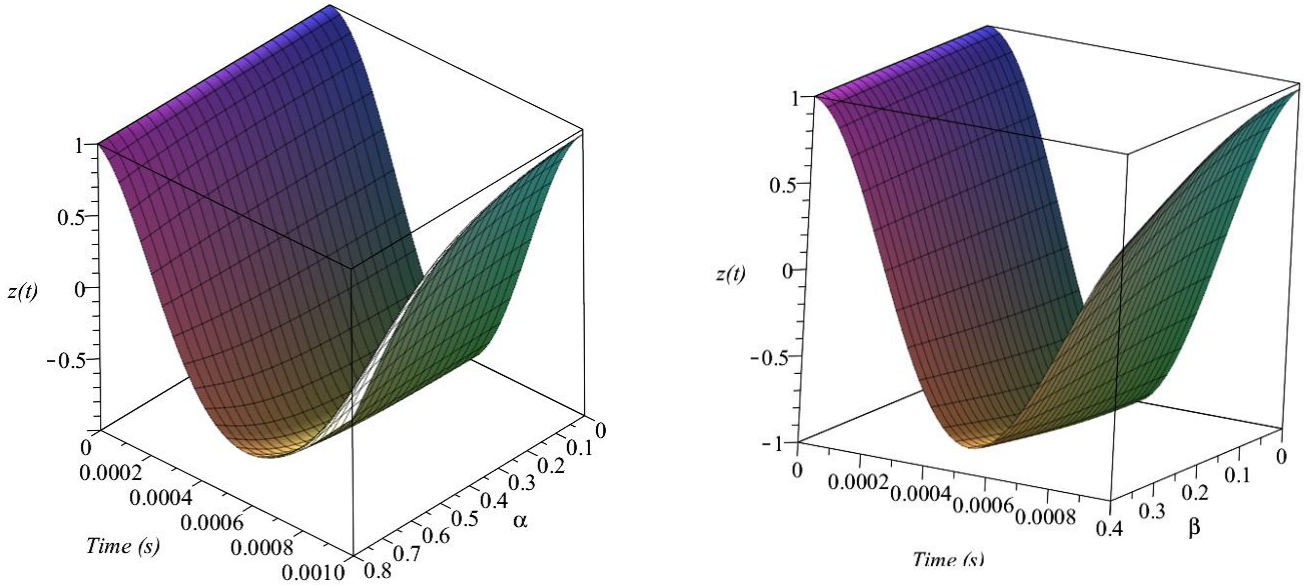

β = 0.2 **α=0.4**

Fig. 4. The deformation response of the beam with (a) a constant crack position ratio (β = 0.2) and varying crack depth ratios, and (b) a constant crack depth ratio (α = 0.4) and varying crack position ratios.

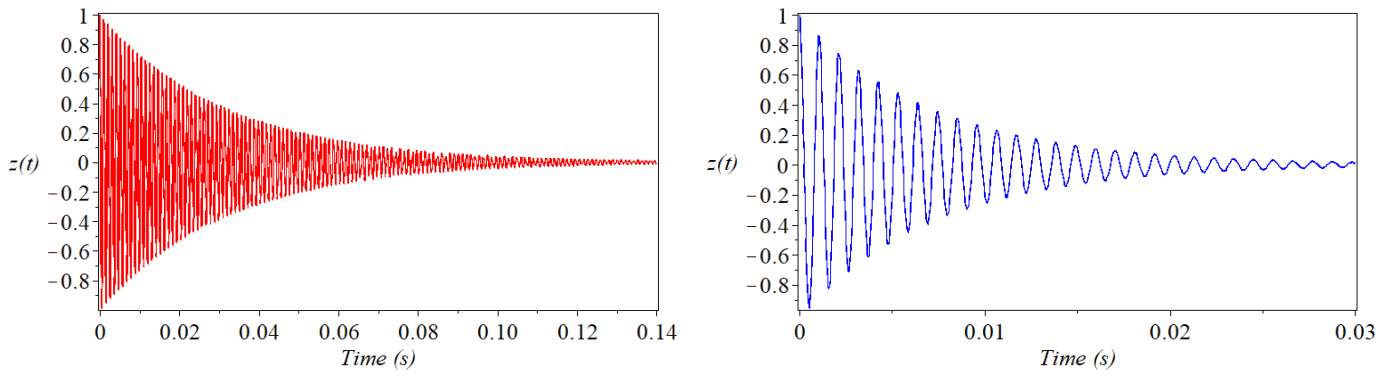

(a) (b)

Fig. 5. The beam deformation response of the crack position ratio β = 0.2 and dual crack depth ratios of (a) α=0.2, and (b) α=0.4.

One major advantage of the given analytical method is its capability to estimate the system's damping due to the crack. Fig. 6 illustrates how the damping factor varies with the crack position ratio at dissimilar crack depth ratios. The figure indicates that the system damping reaches its peak for a specific crack depth when the crack is situated at the beam's midpoint. Consequently, the

damping factor is responsive to the crack's depth and location.

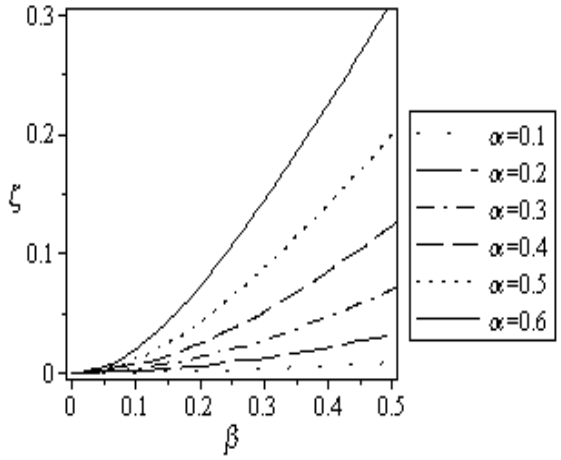

Fig. 6. Damping factor variation of the vibration flexural cracked beam concerning the crack position ratio for various crack depth ratios.

To verify the analytical solution for the beam for the crack parameters $\alpha = 0.4$ and $\beta = 0.2$, the motion equation is resolved numerically via the fourth-order Runge-Kutta technique, with the results presented in Table 1. The primary conditions match those used in the analytical case. The comparison of HPM and numerical results shows strong agreement between the analytical and numerical solutions. It's important to note that the beam's damping factor is not included in numerical methods; thus, an assumed value is necessary. In this context, some researchers have taken values of 0.01 and 0.15 for the damping factor in the vibration analysis of flexural fatigue-cracked beams. As previously mentioned, the system's damping relies on the crack parameters, and the damping factor for a fatigue-fractured beam changes based on crack depth and location. Consequently, the damping factor is derived from the suggested analytical method and applied in the numerical analysis to enhance the accuracy of the numerical method [21].

Table 1. Comparison of the free vibration response of the crack parameters $\beta = 0.2$ and $\alpha = 0.4$ measured from HPM and numerical model.

Time	Displacement (cm)		Velocity (cm/s)	
	Numerical result	(HPM)	Numerical result	(HPM)
0	1	1	0	0
0.001	0.796182	0.803836	2020.033	1907.988
0.005	-0.20705	-0.19625	2773.582	2796.619
0.01	-0.19011	-0.19387	-991.598	-965.217
0.05	8.49E-04	8.58E-04	3.231528	3.10251
0.1	4.32E-07	4.507453432 E-07	5.55E-03	5.446 E-03
0.5	8.90E-12	7.656194548 E-031	-1.07E-07	-5.1E-27
1	-9.84E-12	-9.7E-62	5.06E-08	-7.6E-57

To ensure a legitimate analytical closed-form solution, $\Delta C/C$ must be less than 1.5. Consequently, the shaded area defines the allowable variation limits for the crack parameters (see Fig. 7). The crack terms of the referenced beams are situated within the hatched area. Thus, the analytical solutions acquired are considered valid. To evaluate the accuracy of the results produced by the proposed analytical solution, a comparison is made with the experimental results presented by Chondros et al. [34]. The crack is situated at the center of the bending beam (with assumption $\beta = 0.5$); the suggested analytical method applies to both the breathing and the open crack models.

The solid curve in Fig. 8 illustrates how the fundamental frequency ratio changes for the transverse dynamic vibration of a pinned-supported beam with a breathing crack situated at the midpoint. This variation is plotted against the depth of the crack ratios. In Fig. 8, the experimental results reported by Chondros et al. [34]. The solid curve comparison with the experimental data shows that the proposed method's results agree with the experimental findings reported in the literature. Furthermore, this figure illustrates that the frequency decrease in the open crack mode for a specific crack location ratio is more significant than that in the breathing model. This finding has been established earlier [18].

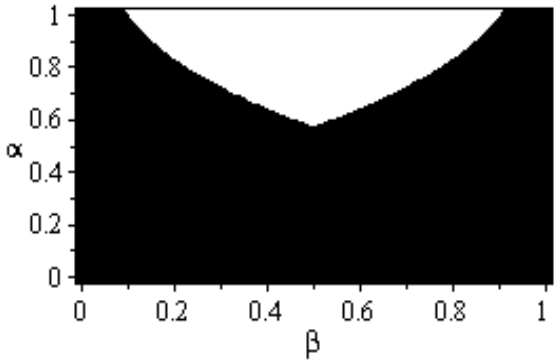

Fig. 7. The area of the flexural crack terms necessary for acquiring a legitimate analytical solution for the vibration analysis of an aluminum-pinned supported beam measuring 7 × 23 × 235 mm³.

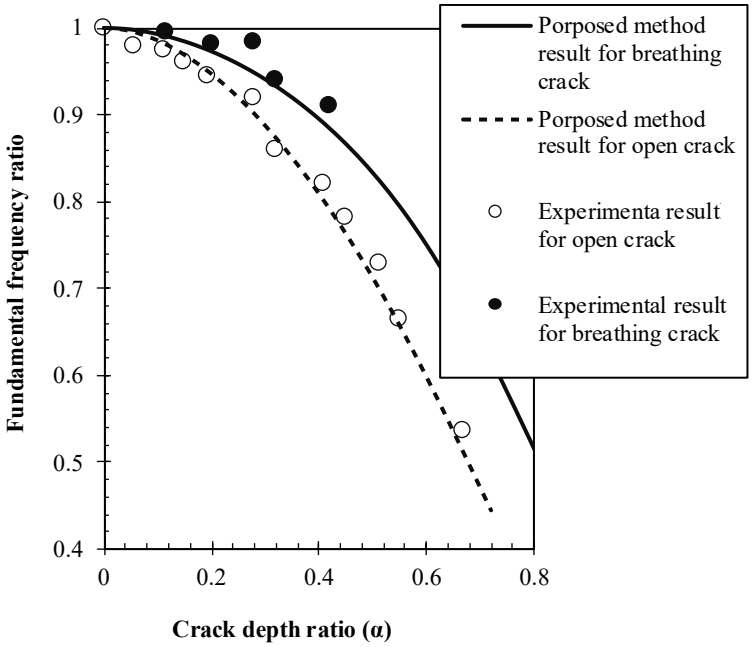

Fig. 8. The variation in the dominant frequency ratio of a cracked pinned-supported bending beam compared to the depth ratio for the crack in the position ratio β = 0.5.

5. Conclusion

This study introduces an analytical alternative novel technique for analyzing the vibrations of a flexural cracked beam. The cracked beam behaves as a nonlinear SDOF structure, with nonlinearity stemming from the crack's breathing behavior. The GE is addressed using the perturbation technique. The solution is valid across a broad spectrum of crack parameters, mechanical characteristics of the beam, and geometric dimensions. This approach estimates the cracked beam's damping ratio due to the crack's existence.

The findings reveal that the crack's depth and location influence the damping factor. Moreover, the super harmonics of the dominant frequency in the response spectra of the cracked beam illustrate its nonlinear dynamic behavior, potentially serving as an indicator of cracks in structural health monitoring applications.

A numerical method is employed alongside the proposed approach to confirm the analytical findings. The free vibration of the flexural cracked beam, calculated using the analytical approach at a specific crack depth and position, matches the numerical results. The outcomes confirm that the solution is consistent with the analytical numerical response.

To confirm the results, a plot of the fundamental frequency ratio against the crack depth ratio for a given crack location ratio is generated according to the breathing flexural crack model, juxtaposed with the experimental findings from the literature. The results indicate compatibility with similar experimental data.

Statements & declarations

Author contributions

Ali Asgari: Conceptualization, Investigation, Formal analysis, Software, Validation, Resources, Writing - Original Draft , Methodology, Writing - Review & Editing, Original Draft,.

Alireza Khabiri: Writing - Review & Editing.

Funding

Funding information is not available.

Declaration

The authors declare that they have no known competing financial interests or personal relationships that could have appeared to influence the work reported in this paper.

Data availability

Data will be made available on request.

References

[1] Khabiri, A., Asgari, A., Taghipour, R., Bozorgnasab, M., Aftabi-Sani, A., Jafari, H. Analysis of Fractional Euler-Bernoulli Bending Beams Using Green's Function Method. Alexandria Engineering Journal, 2024; 106: 312–327. doi:10.1016/j.aej.2024.07.023.

[2] Bahreini, A., Asgari, A., Khabiri, A., Taghipour, R. Analysis of Plane Multi-Span Frames with the Analytical Method of Force-Displacement Combination. Sharif Journal of Civil Engineering. doi:10.24200/j30.2024.64303.3318.

[3] Asgari, A., Ganji D. D., Davodi A. G. Extended tanh method and exp-function method and its application to (2+1)-dimensional dispersive long wave nonlinear equations. Journal of the Applied Mathematics, Statistics and Informatics, 2010; 6: 61–72.

[4] Ganguly, S. Methodologies for Modeling and Identification of Breathing Crack: A Review. MethodsX, 2023; 11: 102420. doi:10.1016/j.mex.2023.102420.

[5] Behvar, A., Haghshenas, M., Djukic, M. B. Hydrogen Embrittlement and Hydrogen-Induced Crack Initiation in Additively Manufactured Metals: A Critical Review on Mechanical and Cyclic Loading. International Journal of Hydrogen Energy, 2024; 58: 1214–1239. doi:10.1016/j.ijhydene.2024.01.232.

[6] Sangid, M. D. The Physics of Fatigue Crack Initiation. International Journal of Fatigue, 2013; 57: 58–72. doi:10.1016/j.ijfatigue.2012.10.009.

[7] Faverjon, B., Sinou, J. J. Identification of an Open Crack in a Beam Using an a Posteriori Error Estimator of the Frequency Response Functions with Noisy Measurements. European Journal of Mechanics, A/Solids, 2009; 28 (1): 75–85. doi:10.1016/j.euromechsol.2008.02.006.

[8] Lam, H. F., Ng, C. T., Veidt, M. Experimental Characterization of Multiple Cracks in a Cantilever Beam Utilizing Transient Vibration Data Following a Probabilistic Approach. Journal of Sound and Vibration, 2007; 305 (1–2): 34–49. doi:10.1016/j.jsv.2007.03.028.

[9] Chati, M., Rand, R., Mukherjee, S. Modal Analysis of a Cracked Beam. Journal of Sound and Vibration, 1997; 207 (2): 249–270. doi:10.1006/jsvi.1997.1099.

[10] Chondros, T. G. The Continuous Crack Flexibility Model for Crack Identification. Fatigue and Fracture of Engineering Materials and Structures, 2001; 24 (10): 643–650. doi:10.1046/j.1460-2695.2001.00442.x.

[11] Loya, J. A., Rubio, L., Fernández-Sáez, J. Natural Frequencies for Bending Vibrations of Timoshenko Cracked Beams. Journal of Sound and Vibration, 2006; 290 (3–5): 640–653. doi:10.1016/j.jsv.2005.04.005.

[12] Ke, L. L., Yang, J., Kitipornchai, S., Xiang, Y. Flexural Vibration and Elastic Buckling of a Cracked Timoshenko Beam Made of Functionally Graded Materials. Mechanics of Advanced Materials and Structures, 2009; 16 (6): 488–502. doi:10.1080/15376490902781175.

[13] Friswell, M. I., Penny, J. E. T. A simple nonlinear model of a cracked beam. In: Proceedings of the International Modal Analysis Conference; 1992 Feb 3–7; California (US).

[14] Sinha, J. K., Friswell, M. I., Edwards, S. Simplified Models for the Location of Cracks in Beam Structures Using Measured Vibration Data. Journal of Sound and Vibration, 2002; 251 (1): 13–38. doi:10.1006/jsvi.2001.3978.

[15] Kisa, M., Brandon, J. Effects of Closure of Cracks on the Dynamics of a Cracked Cantilever Beam. Journal of Sound and Vibration, 2000; 238 (1): 1–18. doi:10.1006/jsvi.2000.3099.

[16] Rytter A. Vibrational based inspection of civil engineering structures [PhD thesis]. Aalborg (DK): University of Aalborg; 1993.

[17] Abraham, O. N. L., Brandon, J. A. The Modelling of the Opening and Closure of a Crack. Journal of Vibration and Acoustics, Transactions of the ASME, 1995; 117 (3): 370–377. doi:10.1115/1.2874463.

[18] Cheng, S. M., Wu, X. J., Wallace, W., Swamidas, A. S. J. Vibrational Response of a Beam with a Breathing Crack. Journal of Sound and Vibration, 1999; 225 (1): 201–208. doi:10.1006/jsvi.1999.2275.

[19] Ariaei, A., Ziaei-Rad, S., Ghayour, M. Vibration Analysis of Beams with Open and Breathing Cracks Subjected to Moving Masses. Journal of Sound and Vibration, 2009; 326 (3–5): 709–724. doi:10.1016/j.jsv.2009.05.013.

[20] Douka, E., Hadjileontiadis, L. J. Time-Frequency Analysis of the Free Vibration Response of a Beam with a Breathing Crack. NDT and E International, 2005; 38 (1): 3–10. doi:10.1016/j.ndteint.2004.05.004.

[21] Loutridis, S., Douka, E., Hadjileontiadis, L. J. Forced Vibration Behaviour and Crack Detection of Cracked Beams Using Instantaneous Frequency. NDT and E International, 2005; 38 (5): 411–419. doi:10.1016/j.ndteint.2004.11.004.

[22] Zhang, W., Testa, R. B. Closure Effects on Fatigue Crack Detection. Journal of Engineering Mechanics, 1999; 125 (10): 1125–1132. doi:10.1061/(asce)0733-9399(1999)125:10(1125).

[23] Bovsunovsky, A. P., Surace, C. Considerations Regarding Superharmonic Vibrations of a Cracked Beam and the Variation in Damping Caused by the Presence of the Crack. Journal of Sound and Vibration, 2005; 288 (4–5): 865–886. doi:10.1016/j.jsv.2005.01.038.

[24] Curadelli, R. O., Riera, J. D., Ambrosini, D., Amani, M. G. Damage Detection by Means of Structural Damping Identification. Engineering Structures, 2008; 30 (12): 3497–3504. doi:10.1016/j.engstruct.2008.05.024.

[25] Dimarogonas, A. D. Vibration of Cracked Structures: A State of the Art Review. Engineering Fracture Mechanics, 1996; 55 (5): 831–857. doi:10.1016/0013-7944(94)00175-8.

[26] Rezaee, M., Hassannejad, R. Free Vibration Analysis of Simply Supported Beam with Breathing Crack Using Perturbation Method. Acta Mechanica Solida Sinica, 2010; 23 (5): 459–470. doi:10.1016/S0894-9166(10)60048-1.

[27] Reta, A. K., Taube, C., Morgenthal, G. Structural Condition Assessment of Cracked RC Beams Based on Digital Crack Measurements. Engineering Structures, 2025; 323: 119211. doi:10.1016/j.engstruct.2024.119211.

[28] Meiramov, D., Ju, H., Seo, Y., Lee, D. Correlation between Deflection and Crack Propagation in Reinforced Concrete Beams. Measurement: Journal of the International Measurement Confederation, 2025; 240: 115527. doi:10.1016/j.measurement.2024.115527.

[29] Dimarogonas, A. D., Paipetis, S. A. Analytical Methods in Rotor Dynamics.; Springer Science & Business Media: Dordrecht, Netherlands, 1983; doi:10.1007/978-94-007-5905-3.

[30] Chondros, T. G., Dimarogonas, A. D., Yao, J. A Continuous Cracked Beam Vibration Theory. Journal of Sound and Vibration, 1998; 215 (1): 17–34. doi:10.1006/jsvi.1998.1640.

[31] Kranz, R. L. Microcracks in Rocks: A Review. Tectonophysics, 1983; 100 (1–3): 449–480. doi:10.1016/0040-1951(83)90198-1.

[32] Shaw, S. Vibrations in mechanical systems: analytical methods and applications. Berlin (DE): Springer Science & Business Media; 1989. Vol. 31. doi:10.1137/1031116.

[33] Clough, R. W., Penzien, J. Dynamics of structures. Berkeley (US): Computers & Structures, Inc.; 1975.

[34] Chondros, T. G., Dimarogonas, A. D., Yao, J. Vibration of a Beam with a Breathing Crack. Journal of Sound and Vibration, 2001; 239(1): 57–67. doi:10.1006/jsvi.2000.3156.